Oligomerization state of the DNA fragmentation factor in normal and apoptotic cells

Delphine Lechardeur, S. Dougaparsad, C. Nemes, G. L. Lukacs

THE JOURNAL OF BIOLOGICAL CHEMISTRY VOL. 280, NO. 48, pp. 40216–40225, December 2, 2005

Oligomerization State of the DNA Fragmentation Factor in Normal and Apoptotic Cells*[S]

Received for publication, February 28, 2005, and in revised form, September 7, 2005 Published, JBC Papers in Press, October 3, 2005, DOI 10.1074/jbc.M502220200

Delphine Lechardeur, Sam Dougaparsad, Csilla Nemes, and Gergely L. Lukacs[1]

From the Program in Cell and Lung Biology, Hospital for Sick Children Research Institute and Department of Laboratory Medicine and Pathobiology, University of Toronto, Toronto, Ontario M5G 1X8, Canada

The caspase-activated DNase (CAD) is the primary nuclease responsible for oligonucleosomal DNA fragmentation during apoptosis. The DNA fragmentation factor (DFF) is composed of the 40-kDa CAD (DFF40) in complex with its cognate 45-kDa inhibitor (inhibitor of CAD: ICAD or DFF45). The association of ICAD with CAD not only inhibits the DNase activity but is also essential for the co-translational folding of CAD. Activation of CAD requires caspase-3-dependent proteolysis of ICAD. The tertiary structures of neither the inactive nor the activated DFF have been conclusively established. Whereas the inactive DFF is thought to consist of the CAD/ICAD heterodimer, activated CAD has been isolated as a large (>MDa) multimer, as well as a monomer. To establish the subunit stoichiometry of DFF and some of its structural determinants in normal and apoptotic cells, we utilized size-exclusion chromatography in combination with co-immunoprecipitation and mutagenesis techniques. Both endogenous and heterologously expressed DFF have an apparent molecular mass of 160–190 kDa and contain 2 CAD and 2 ICAD molecules $(CAD/ICAD)_2$ in HeLa cells. Although the N-terminal (CIDE-N) domain of CAD is not required for ICAD binding, it is necessary but not sufficient for ICAD homodimerization in the DFF. In contrast, the CIDE-N domain of ICAD is required for CAD/ICAD association. Using bioluminescence resonance energy transfer (BRET), dimerization of ICAD in DFF was confirmed in live cells. In apoptotic cells, endogenous and exogenous CAD forms limited oligomers, representing the active nuclease. A model is proposed for the rearrangement of the DFF subunit stoichiometry in cells undergoing programmed cell death.

Apoptosis or programmed cell death ensures the elimination of unwanted cells during normal development and tissue homeostasis without affecting the viability of adjacent cells. At the molecular level, apoptosis comprises a cascade of proteolytic events mediated by a family of cysteine-aspartate proteases, the caspases, involved in both the signaling and the execution phase of cell death (1). Apoptotic cells undergo preprogrammed morphological changes, reflected by cell and nuclear shrinkage, chromatin condensation, and apoptotic body formation, ultimately engulfed by scavenger cells (2). One of the biochemical hallmarks of apoptosis is the cleavage of nuclear DNA into oligonucleosome-sized fragments, or DNA fragmentation, a mechanism thought to be essential for preventing autoimmune diseases and horizontal gene transfer (3, 4).

Although, several nucleases (*e.g.* endonuclease G, AIF, DNase I, and DNase II) have been implicated in the degradation of genomic DNA during apoptosis (5), the 40-kDa caspase-activated DNase (CAD)[2] or DNA fragmentation factor 40 (DFF40) is considered to account for the majority of nuclease activity responsible for chromosomal DNA fragmentation (6, 7). In proliferating cells, CAD is expressed as an inactive nuclease by binding to the 45-kDa inhibitor of CAD (ICAD or DFF45), forming the heterodimeric DNA fragmentation factor (DFF) (8–13). According to the original hypothesis, inactive DFF was confined to the cytoplasm (10) but more recent evidence indicates that DFF is constitutively targeted into the nucleus. Two nuclear localization signals (NLSs) at the C termini of CAD and ICAD co-operate for the nuclear uptake of the DFF (15–17). A 35-kDa splicing variant of ICAD (ICAD-S or DFF35), lacking the C-terminal domain is also ubiquitously expressed, but does not appear to interact with CAD (16). During apoptosis, caspase-3 and -7-mediated cleavage of ICAD provokes the release and activation of CAD, leading to the generation of double-stranded breaks in internucleosomal chromatin regions (18).

Several pieces of evidence support the role of protein-protein interactions in the regulation of CAD activity at the co-translational and post-translational levels (3). ICAD appears to be essential for the co-translational folding of CAD in concert with Hsp/Hsc70 and Hsp40 (19). Biosynthesis of CAD in the absence of ICAD fails to produce folded CAD in prokaryotic and eukaryotic expression systems (20). In addition, complex formation of CAD with ICAD inhibits the nuclease activity providing a safeguard mechanism against inadvertent activation of the DNase (10, 20, 21). A variety of DNA-binding proteins, such as histone H1, high mobility group (HMG) 1/2, and topoisomerase II have been invoked in the stimulation of CAD *in vitro*, as allosteric activators and/or by influencing the DNA conformation (9, 13, 22, 23).

Both CAD and ICAD are composed of an N-terminal regulatory domain homologous to the N terminus of the pro-apoptotic CIDE (cell-inducing DFF45-like effector) A/B proteins (24). The CIDE-N domains of CAD and ICAD have been shown to mediate their heterodimerization in DFF (24). The oligomerization tendency of the CIDE-N domain also provided a plausible explanation for the observation that the CAD/ICAD complex is expressed as a heterodimer (apparent molecular mass 85 kDa) (8, 13, 21), determined by size-exclusion chromatography. The quaternary structure of activated DFF is less well established. Following the caspase-3-dependent proteolysis of ICAD, CAD was identified in large homo-oligomers (>1 MDa), constituting the active form of the DNase (13, 25–27). Whereas the activated CAD, purified from lymph

* This work was supported by a grant from the Canadian Institute of Health Research and the Premier Research Excellence Award (to G. L. L.). The costs of publication of this article were defrayed in part by the payment of page charges. This article must therefore be hereby marked "*advertisement*" in accordance with 18 U.S.C. Section 1734 solely to indicate this fact.

[S] The on-line version of this article (available at http://www.jbc.org) contains supplemental Figs. S1 and S2.

[1] To whom correspondence should be addressed: Hospital for Sick Children, 555 University Ave., Toronto, Ontario M5G 1X8, Canada. Tel.: 416-813-5125; E-mail: glukacs@sickkids.ca.

[2] The abbreviations used are: CAD, caspase-activated DNase; BRET, bioluminescence resonance energy transfer; BRET^2, a modified version of BRET; CIDE, cell-inducing DFF45-like effector; DFF, DNA fragmentation factor; ICAD, inhibitor of caspase-activated DNase; PBS, phosphate-buffered saline; FITC, fluorescein isothiocyanate; TRITC, tetramethylrhodamine isothiocyanate; HA, hemagglutinin; Ab, antibody.

node cells, was monomeric (10), recombinant DFF showed multimodal size distribution with the prevalence of large oligomers (21). Large homo-oligomers as representative of activated endogenous CAD were detected by native pore-exclusion limit electrophoresis as well (21, 27). Notably, the crystal structure of CAD suggested a homodimeric configuration in the form of molecular scissors of DNA (28).

To assess the composition of endogenous and exogenous DFF in normal and apoptotic cells, we used complementary *in vitro* and *in vivo* approaches. Our results, obtained by size-exclusion chromatography, co-immunoprecipitation, and the bioluminescence fluorescence energy transfer (BRET) technique suggest that the inactive DFF contains two ICAD and two CAD molecules. Whereas the CIDE-N domain of CAD is necessary but not sufficient for CAD-dependent homodimerization of ICAD in the inactive DFF, it is not required for ICAD/CAD dimerization. Following the proteolysis of ICAD *in vivo*, the molecular mass of both endogenous and heterologously expressed CAD is consistent with the formation of dimeric/tetrameric CAD. We propose that conversion of the heterotetrameric DFF into homo-oligomeric CAD contributes to the activation mechanism of DFF in apoptotic cells.

MATERIALS AND METHODS

Plasmid Construction—The cDNA, encoding the human and mouse CADs (hCAD and mCAD) were kindly provided by Dr. R. Halenbeck (Chiron Corp., Emeryville, CA) and Dr. S. Nagata (Department of Genetics, Osaka University Medical School, Osaka, Japan), respectively. The cDNA of human ICAD was isolated by PCR cloning using a cDNa library prepared from CaCo-2 cells (American Type Culture Collection, HTB37) as a template (15). Epitope-tagged CADs and ICADs were obtained as described previously (15). Briefly, hICAD, mCAD, and hCAD were subcloned into the expression plasmid vector pcDNA3 or pcDNA3.1, incorporating in-frame fusion of the coding sequence of the HA, Myc, or the FLAG epitope at either the C or the N terminus. ΔCIDE deletion mutants of mCAD and hICAD were obtained by PCR, amplifying the cDNA fragments encoding amino acid residues 84–344 in mCAD and 83–331 in hICAD. The cDNA fragments were inserted into pcDNA3.1 harboring a Myc tag at the C terminus. hICAD-S expression vector was constructed by PCR and encoded amino acid residues 1–266 of hICAD. The expression plasmid encoding the HA-CAD-EGFP fusion protein (CAD-GFP) was constructed by subcloning the coding region of the HA-CAD into pEGFP-N1 plasmid (BD Biosciences). N- and C-terminal truncations of hCAD were obtained by PCR, and the mutants were subcloned into pEGFP-N1 plasmid as described (29). ICAD-Rluc expression vector was obtained by inserting hICAD lacking its stop codon into the pRluc-N1 (PerkinElmer Life Sciences). GFP^2, the F64L mutant of GFP, was cut out from the pRluc-GFP^2 vector (PerkinElmer Life Sciences) and fused to the C terminus of the hICAD. All constructs were verified by dideoxy chain termination DNA sequencing.

Cell Culture, Transfection, and Induction of Apoptosis—HeLa and COS-1 cells were grown in Dulbecco's modified Eagle's medium supplemented with 10% fetal bovine serum at 37 °C under 5% CO_2 containing air. Transfections were performed with FuGENE (Roche Applied Science), and cells were harvested after 24–48 h. The ratio of CAD/ICAD plasmid DNA was 1:1 or 2:1 in transient transfections. To maintain the DNA/lipid ratio and comparable transfection efficiency, identical levels of the total amount of DNA (8 μg of DNA/24 μl of FuGENE for 10 cm, 60% confluent tissue culture dish) was utilized in different transfections by supplementing the indicated expression vectors with the appropriate amount of pcDNA3.1. Apoptosis was induced with 2 μM staurosporine (Sigma) for 2 h in tissue culture medium.

S-100 Fractions of HeLa Cells and Caspase-3-induced Activation of CAD—Transiently transfected HeLa cells were resuspended in ice-cold hypotonic buffer (20 mM Hepes-KOH, pH 7.5, 10 mM KCl, 1.5 mM $MgCl_2$, 1 mM Na_2EGTA, and 1 mM dithiothreitol) supplemented with 10 μg/ml leupeptin, 10 μg/ml pepstatin, and 1 mM phenylmethylsulfonyl fluoride. After 15 min of incubation on ice, cells were disrupted by 15 strokes in a 2-ml Kontes homogenizer (B pestle, Kontes Glass). The lysates were cleared (15,000 × *g*, 15 min at 4 °C), and insoluble materials were sedimented in a bench-top Beckman ultracentrifuge (100,000 × *g*, 30 min, 4 °C). Aliquots of the S-100 fraction were incubated for 1 h at 21 °C with recombinant human caspase-3 (Calbiochem) at the indicated concentration.

Immunoblotting and Immunoprecipitation—Immunoblotting and immunoprecipitations were performed on cells transiently transfected with the indicated CAD and ICAD constructs. Cells were washed with ice-cold PBS, detached from culture dishes with a non-enzymatic cell dissociation buffer (Invitrogen), and sedimented by centrifugation (2000 × *g*, 5 min at 4 °C). The pellet was resuspended and incubated in lysis buffer (150 mM NaCl, 20 mM Tris-HCl, 0.2% Triton X-100, pH 7.4) containing 10 μg/ml leupeptin, 10 μg/ml pepstatin, and 2 mM phenylmethylsulfonyl fluoride for 10 min at 4 °C. The lysates were cleared by centrifugation (15,000 × *g*, 15 min at 4 °C), and soluble proteins were denatured in Laemmli sample buffer (LSB) or immunoprecipitated from the cell lysates using the indicated antibodies (see below) and protein G-agarose (Sigma). Proteins were eluted from the beads with 2× LSB containing 100 mM β-mercaptoethanol. Lysates and immunoprecipitates were separated by SDS-PAGE and transferred to a nitrocellulose membrane. The following antibodies were used: mouse monoclonal anti-HA.11 (Covance), mouse monoclonal anti-Myc 9E10 (Covance), mouse monoclonal and rabbit polyclonal anti-GFP (Molecular Probes), monoclonal anti-FLAG M2 (Sigma), rabbit polyclonal anti-mCAD (AAP-351, Stressgen), rabbit polyclonal anti-human CAD (BD Pharmingen), and monoclonal anti-Hsc/HSP70 (Calbiochem). The rabbit polyclonal anti-hICAD was prepared and characterized as described (15). Primary antibodies were visualized with horseradish peroxidase-conjugated secondary Abs (Amersham Biosciences) and Supersignal West Pico Stable peroxide solution (Pierce).

Immunostaining—Transfected HeLa cells were plated on glass coverslips, rinsed in phosphate-buffered saline (PBS; 137 mM NaCl, 2.7 mM KCl, 4.3 mM Na_2HPO_4, 1.4 mM KH_2PO_4, pH 7.3), and fixed in PBS containing 4% paraformaldehyde for 15 min. Cells were permeabilized in PBS containing 0.2% Triton X-100 for 5 min, blocked in 0.5% bovine serum albumin, and incubated with the rat monoclonal anti-HA (Roche Applied Science), rabbit anti-Myc (Santa Cruz), and the M2 mouse monoclonal anti-FLAG (Sigma) antibodies, in blocking solution. Primary antibodies were visualized with FITC-conjugated goat anti-rat (Jackson), TRITC-conjugated donkey anti-rabbit (Jackson), and Cy5-conjugated goat anti-mouse (Invitrogen). Triple-stained cells were analyzed with a Zeiss 510 fluorescence laser confocal microscope. Single optical sections were taken consecutively, using the 488-, 543-, and 633-nm laser lines. Control experiments verified that no fluorescence spill-over occurred in any of the cells stained with a single-fluorophore (data not shown). Images were assembled with Adobe Photoshop 7 (Adobe Systems, San Jose, CA).

Gel Filtration Chromatography—HeLa cells were solubilized as described for immunoblotting and immunoprecipitation. Lysates were cleared by ultracentrifugation (100,000 × *g*, 30 min, 4 °C) in a bench-top Beckman ultracentrifuge. The supernatant was loaded on a Superdex 200 HR 10/30 gel filtration column (Amersham Biosciences) equilibrated with 20 mM Tris/HCl, 100 mM NaCl, 5 mM EDTA, 2 mM $MgCl_2$,

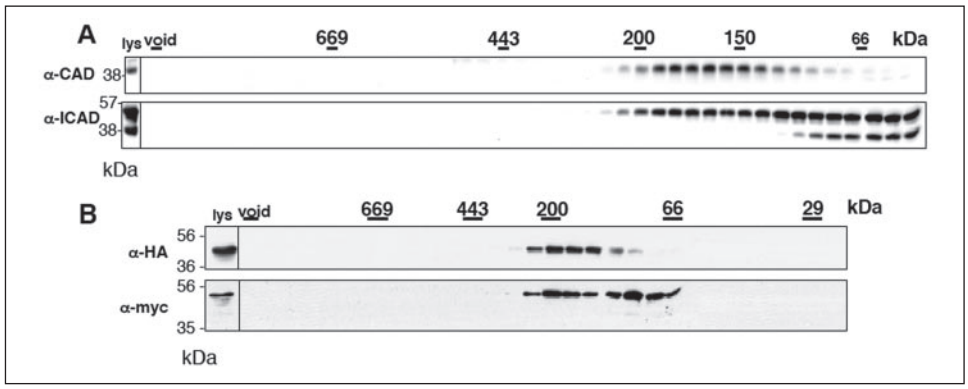

FIGURE 1. **Analysis of the molecular mass of the DFF by size-exclusion chromatography.** Cell lysates obtained from non-transfected (*A*) or CAD-HA/ICAD-Myc-expressing HeLa cells (*B*) were fractionated by size-exclusion chromatography as described under "Materials and Methods." Polypeptides from each fraction were separated by SDS-PAGE. Endogenous and epitope-tagged ICADs and CADs were visualized by Western blot analysis using anti-hCAD, anti-hICAD, anti-HA, and anti-Myc antibodies, as indicated. The elution profile of molecular mass standards was determined in parallel fractionations, and their positions are indicated. 2% of the cell lysates (*lys*) were loaded on the gels.

5 mM dithiothreitol, 15% (v/v) glycerol, pH 7.4 and mounted on a Beckman Gold Nouveau HPLC system (166 pump module, 168 detector). Fractions of 300 μl were collected on ice at a flow rate of 0.2–0.3 ml/min. The following molecular size markers were used to calibrate the gel filtration column after each separation: carbonic anhydrase, 29 kDa; bovine serum albumin, 66 kDa; alcohol dehydrogenase, 150 kDa; β-amylase, 200 kDa; apoferritin, 443 kDa; thyroglobulin, 669 kDa, and blue dextran, 2 MDa (molecular weight marker kit, Sigma). 80 μl from each fraction were subjected to 10% SDS-PAGE followed by Western blot analysis as described in the figure legend.

BRET² Measurement—Bioluminescence resonance energy transfer between ICAD-GFP² and ICAD-Rluc fusion proteins was analyzed on transiently transfected COS-7 cells essentially as described (31). Cells were detached from the culture dishes and suspended in PBS containing 0.1% glucose before addition of the Rluc substrate DeepBlue Colenterazine (DeepBlueC, Packard Biosciences) in 96-well plates (Costar). BRET was monitored by a Polarstar Ultima (BMG Labtech) luminometer. The BRET signal was determined by calculating the ratio of the light emitted by the ICAD-GFP² (500–530 nm) and the light emitted by the ICAD-Rluc (370–450 nm). The values were corrected by subtracting the background signal of non-transfected cells. In each experiment nonspecific BRET² signal of ICAD-GFP co-expressed with Rluc and Rluc alone was also determined.

RESULTS

Contribution of CAD and ICAD to the Formation of DFF in Vivo—To test whether DFF is a heterodimer *in vivo*, as proposed previously (13, 10) the molecular mass of DFF components was determined by size-exclusion chromatography. Triton X-100 (0.2%) not only fully extracted the cellular DFF content, but also preserved the association of CAD and ICAD, as demonstrated by co-immunoprecipitation and immunoblotting studies (data not shown and Ref. 15). In HeLa cell lysates, endogenous CAD was detected as a single polypeptide band with an apparent molecular mass of ~40 kDa by immunoblotting (Fig. 1*A*, *lys*). The polyclonal anti-ICAD Ab recognized both the full-length form (ICAD, ~45 kDa) and its spliced variant, ICAD-S (~35 kDa, Fig. 1*A*, *lys* and Ref. 15).

Western blot analysis of size-fractionated cell extracts revealed that endogenous CAD was associated with a macromolecular complex of ~150–190 kDa (Fig. 1*A*, *top panel*), which was significantly larger than the predicted molecular mass of the CAD/ICAD heterodimer (~72 kDa). Regarding the ICAD elution pattern, two distinct populations could be distinguished. A significant amount of ICAD was co-fractionated with CAD between ~150 and ~190 kDa (Fig. 1*A*, *lower panel*), conceivably because of their complex formation. Immunoreactive CAD, however, was absent from the second population of ICAD, confined between ~45 and ~90 kDa (Fig. 1*A*). This could be explained by the biosynthesis of molar excess of ICAD, unable to bind CAD (Fig. 1*A*). Virtually all the endogenous ICAD-S was fractionated in the absence of CAD with an apparent molecular mass of <70 kDa, consistent with its negligible binding to CAD in the presence of excess ICAD (Fig. 1 and Ref. 17). Similar results were obtained when the chromatography was performed on HeLa S-100 fraction (data not shown).

The Endogenous and Exogenous DFF Has Similar Molecular Mass—The molecular mass of the endogenous DFF (~150–190 kDa) is consistent with the possibility that DFF is composed of more than a single CAD/ICAD heterodimer in dividing cells. This hypothesis is at variance with previous propositions indicating that DFF is a heterodimer (~80 kDa) (13, 10). In an attempt to establish the subunit composition of the DFF, we utilized a panel of epitope-tagged (HA, Myc, and FLAG) CAD and ICAD molecules. As a convention, the N-terminal tag precedes (*e.g.* HA-CAD), whereas the C-terminal tag follows (*e.g.* CAD-HA) the name of the polypeptide.

We have established that ~5-fold overexpression of CAD and ICAD relative to their endogenous level was sufficient to ensure preferential incorporation of tagged molecules into the heterologous DFF (29). Control experiments demonstrated that the tagged CAD and ICAD reproduced the cellular phenotype (constitutive nuclear targeting) and biochemical properties (chaperone function of ICAD, complex formation between ICAD and CAD, and immobilization of activated CAD to the nuclear matrix) of their endogenous counterparts (Refs. 15 and 29 and data not shown).

To validate that the complex formation of epitope-tagged CAD and ICAD was preserved, extracts of HeLa cells, transiently co-expressing CAD-HA and ICAD-Myc, were fractionated by size-exclusion chromatography. The elution profiles of CAD-HA (Fig. 1*B*, *upper panel*) and ICAD-Myc (Fig. 1*B*, *lower panel*) were visualized with the anti-HA and anti-Myc antibodies, respectively. CAD-HA was eluted as a single, ~150–200-kDa peak, similar to that of the endogenous CAD (Fig. 1*A*). ICAD-Myc resided in the same fractions as CAD-HA (Fig. 1*B*, *lower panel*), consistent with their association. A fraction of ICAD-Myc was eluted at ~70–100 kDa, likely representing uncomplexed protein, similar to that observed for the endogenous mammalian ICAD as well as *Drosophila* dICAD (21, 30).

The observation that the endogenous and exogenous CADs have similar chromatographic profiles confirmed that epitope-tagged CAD and ICAD preserved their oligomerization propensity and were suitable for investigating the subunit stoichiometry of DFF. These data also imply that the DFF either incorporates more than one CAD/ICAD heterodimer, or associates with other polypeptides *in vivo*.

Two ICAD Molecules Are Incorporated into the DFF—If DFF consists of two CAD/ICAD heterodimers in non-apoptotic cells, co-expression of ICAD-Myc and HA-ICAD should be observed in ~50% of the exog-

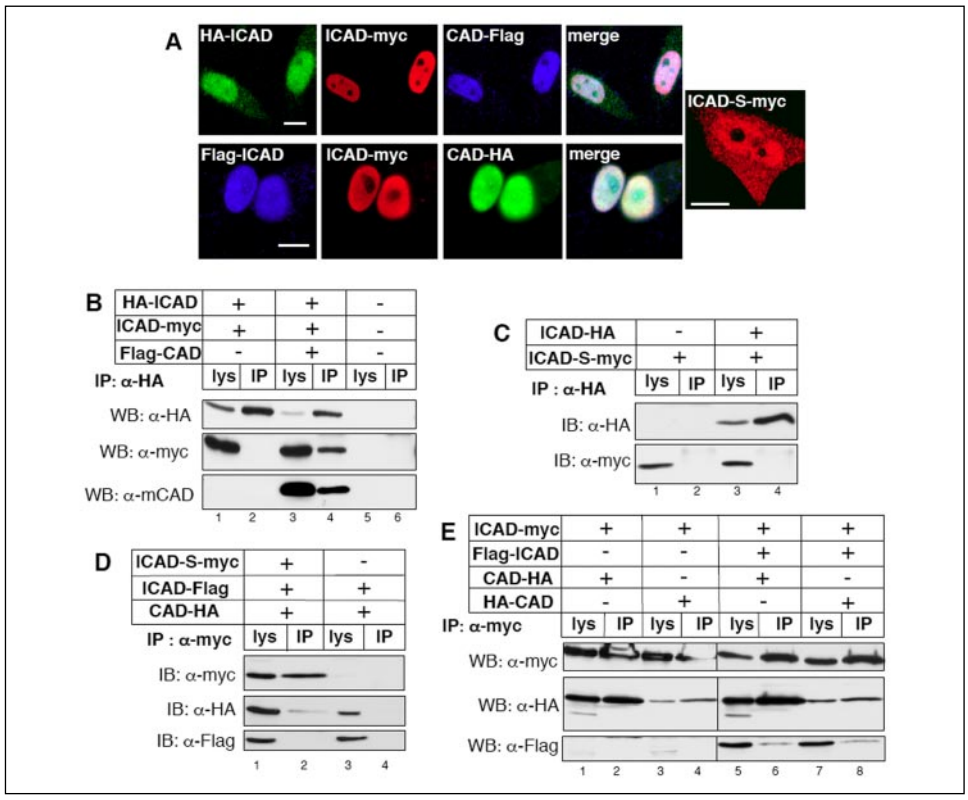

FIGURE 2. **DFF contains two ICADs.** *A*, triple-tagged DFF is nuclear. Indirect immunostaining of HeLa cells expressing 2 epitope-tagged ICADs together with tagged CAD or ICAD-S-Myc are indicated. The anti-tag primary antibodies were visualized with FITC-, TRITC-, and Cy5-conjugated secondary antibodies as described under "Materials and Methods." *Bar*, 10 μm. *B*, association of ICAD/ICAD in DFF. HeLa cells were co-transfected with HA-ICAD and ICAD-Myc in the absence or presence of the FLAG-tagged mouse CAD. Non-transfected cells were used as controls. Immunoprecipitates (*IP*), obtained with anti-HA antibody, were probed by Western blotting (*WB*) with indicated antibodies and enhanced chemiluminescence. 5% of the total lysates (*lys*) were loaded to verify the expression of tagged ICADs and CAD. *C* and *D*, ICAD-S does not associate with ICAD. HeLa cells were co-transfected with ICAD-HA and ICAD-S-Myc (*C*) or ICAD-FLAG, and ICAD-S-Myc in the presence of CAD-HA (*D*). Association was probed as described in *B*. *E*, association of ICAD/ICAD in the DFF. CAD-dependent ICAD/ICAD association was probed in HeLa cells as described in *B*.

enous DFF complexes. To test this prediction, it was necessary to transiently co-express ICAD-Myc and HA-ICAD (or ICAD-Myc and FLAG-ICAD) in the presence of FLAG-CAD (or CAD-HA) and to evaluate their oligomerization with the co-immunoprecipitation technique. To this end, we demonstrated first that co-expression of CAD and ICAD molecules with three different epitope tags did not interfere with their nuclear targeting by immunostaining (Fig. 2*A*). Most of the cells contained the three constructs, suggesting that they had comparable transfectional and translational efficiencies (Fig. 2*A* and data not shown). To demonstrate possible interactions between ICAD-Myc and HA-ICAD, immunoprecipitates obtained with anti-HA antibody were probed for the presence of ICAD-Myc, HA-ICAD, and FLAG-CAD, using the respective anti-tag antibody. Both ICAD-Myc and FLAG-CAD were detected in the immunoisolated HA-ICAD (Fig. 2*B*, *lane 4*). Nonspecific association with protein G-agarose can be precluded, because no ICAD-Myc was pulled-down in the absence of FLAG-CAD (Fig. 2*B*, *lane 2*). Furthermore, dimerization of ICAD with itself (represented by the formation of ICAD-Myc/HA-ICAD complex) or with ICAD-S was negligible in the absence of exogenous CAD (Fig. 2, *B*, *lane 2* and *D*, *lane 4*).

ICAD-S-Myc was co-immunoprecipitated with CAD inefficiently in the presence of CAD-HA and ICAD-FLAG (Fig. 2*D*, *lane 2*, *middle panel*). ICAD-S was also unable to bind to ICAD (Fig. 2*D*, *lane 2*, *middle panel*), ruling out the possibility that the splice variant participates in the DFF formation. ICAD molecules bearing different tags (ICAD-Myc and FLAG-ICAD) were also co-precipitated in the presence of HA-CAD or CAD-HA, using anti-Myc and anti-FLAG antibodies (Fig. 2*E*, *lanes 6* and *8*). Similar results were obtained with the human version of CAD (data not shown).

Detection of ICAD-ICAD Interaction by BRET^2 in Vivo—ICAD-ICAD interaction was confirmed by utilizing the BRET technique, capable of demonstrating the proximity (<100 Å) of interacting proteins in living cells (31). First we verified that ICAD fusion proteins, containing the acceptor fluorophore GFP^2 (ICAD-GFP^2) and *Renilla luciferase* (ICAD-Rluc), behaved as their endogenous counterparts. Both ICAD fusions were indeed targeted to the nucleus with CAD-HA (Fig. 3*A*), supported the co-translational folding of CAD-HA similarly to ICAD-Myc (Fig. 3*B*) and were co-precipitated with CAD-HA (data not shown).

Several observations indicate that the BRET signal between ICAD-GFP^2 and ICAD-Rluc is specific upon their co-expression in HeLa cells in the presence of the DeepBlueC substrate (Fig. 3*B*). First, minimal or no energy transfer was observed when ICAD-GFP^2 was co-expressed with Rluc instead of ICAD-Rluc at comparable expression levels (Fig. 3, *B* and C). Second, co-expression of exogenous CAD enhanced the BRET signal by 3-fold (Fig. 3, *C* and *D*), confirming that ICAD dimerization is substantially facilitated by CAD-HA. The small BRET signal in the absence of exogenous CAD, most likely, reflects the limited oligomerization of ICAD with endogenous CAD (Fig. 3*D*). Finally, the energy transfer efficiency increased as a function of increasing amount of ICAD-GFP^2 at constant ICAD-Rluc concentration, both in the presence and absence of CAD-HA, consistent with the notion that the signal was derived from specific interaction between the two ICAD molecules (Fig. 3*C*). These *in vivo* and *in vitro* results, collectively, suggest that the DFF complex contains at least 2 ICAD molecules in non-apoptotic cells.

The Inactive DFF Harbors Two CAD Molecules—To evaluate whether more than 1 CAD molecule was incorporated into the DFF complex, we resorted to the co-immunoprecipitation technique. First, the nuclear expression of the three differentially tagged CAD and ICAD molecules was assessed. According to indirect immunostaining, CAD-HA/CAD-Myc/ICAD-FLAG, HA-CAD/CAD-Myc/ICAD-FLAG, and CAD-HA/CAD-FLAG/ICAD-Myc were efficiently co-expressed in HeLa cell nuclei (Fig. 4*A*). Following the co-expression of CAD-Myc and CAD-HA with ICAD, CAD-HA was isolated by immunoprecipitation. The precipitates were probed with anti-Myc and anti-ICAD antibodies (Fig. 4*B*). Both CAD-Myc and ICAD were associated with

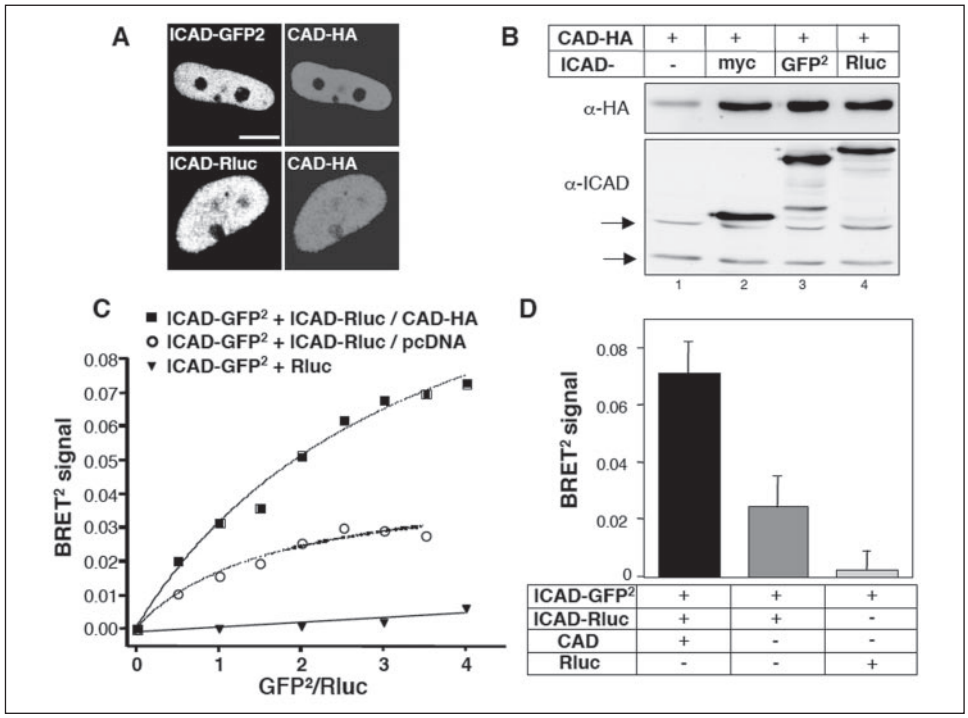

FIGURE 3. **Detection of ICAD-ICAD interaction by BRET² *in vivo*.** *A* and *B*, ICAD-GFP² and ICAD-Rluc fusion proteins behave similar to native ICAD. *A*, ICAD-GFP² and ICAD-Rluc co-expressed with CAD are targeted to the nucleus. HeLa cells co-transfected with ICAD-GFP²/CAD-HA or ICAD-Rluc/CAD-HA were immunostained with anti-HA or anti-ICAD antibodies as described under "Materials and Methods." *Bar*, 10 μm. *B*, ICAD-GFP² and ICAD-Rluc associate with CAD. Cell lysates from transiently transfected cells were probed by Western blotting. *Arrows* indicate endogenous ICAD and ICAD-S. *C*, bioluminescence energy transfer between ICAD-GFP² and ICAD-Rluc is potentiated by exogenous CAD. COS-7 cells were transiently transfected with constant concentration of ICAD-Rluc and increasing concentrations of ICAD-GFP² in the presence or absence of CAD-HA. The amount of ICAD cDNA was kept constant by the addition of non-tagged ICAD to maintain a 1:1 ratio of CAD:ICAD cDNA. Co-transfection of ICAD-GFP² and Rluc were performed at the indicated ratios as negative controls. The BRET signal was measured in the presence of DeepblueC, as described under "Materials and Methods." Data are means of duplicate measurements from a representative experiment of at least three independent studies. *D*, BRET signal between ICAD-GFP² and ICAD-Rluc. Cells were transfected and at the ICAD-GFP²:ICAD-Rluc ratio of 4:1, the BRET signal was determined as in *C*. Means ± S.E., $n = 3–4$.

CAD-HA (Fig. 4*B*, *lane 2*). Similar results were obtained when HA-CAD and CAD-Myc were used (Fig. 4*C*, *lane 2*), indicating that at least 2 CADs are incorporated into heterologously expressed DFF. Because CAD cannot be expressed in the absence of associated ICAD, the molecular mass of DFF (~150–190 kDa) (Fig. 1), measured by size-exclusion chromatography, most likely, reflects the predicted mass (~170 kDa) of a tetrameric DFF, consisting of $(CAD/ICAD)_2$.

We could not resort to BRET to confirm CAD/CAD interaction in living cells, since GFP²/RlucCAD fusion proteins aggregated and were predominantly excluded from the nucleus (data not shown). Nevertheless, the following observations support the notion that the tetramerization of the epitope-tagged DFF cannot be attributed to nonspecific association of 2 CAD/ICAD dimers *in vitro*, but is rather because of their assembly *in vivo*. First, the apparent molecular mass of the CAD-containing complexes was similar for both the endogenous and the heterologously expressed DFFs (Fig. 1). Second, ICAD overexpression without CAD did not lead to its oligomerization (Fig. 2*B*, *lane 2*). Finally, rearrangement of DFF constituents could not be observed after mixing differentially tagged CAD/ICAD *in vitro*. This was proven by first preparing lysates from HeLa cells expressing CAD-FLAG/HA-ICAD and CAD-FLAG/ICAD-Myc. Then, these lysates were combined, and association of ICADs was measured. We were unable to co-precipitate ICAD-Myc with HA-ICAD after combining the two lysates, despite high levels of ICAD expression (Fig. 4*D*). Mixing cell lysates with two different epitope-tagged CAD (CAD-HA/FLAG-ICAD and CAD-Myc/FLAG-ICAD) also provided negative results (Fig. 3*E*). No interaction between CAD-HA and CAD-Myc was detected, supporting our conclusion that assembly of DFF is achieved *in vivo* and cannot be attributed to postlysis association of DFF subunits. Although we are unable to distinguish whether DFF assembles by the dimerization of CAD_2 and $ICAD_2$ or the heterodimeric CAD/ICAD, in light of the co-translational association of CAD and ICAD (19), we favor the latter scenario.

The Role of the CIDE-N Domain in the Oligomerization of DFF—The model that DFF contains 2 CAD and 2 ICAD molecules raised the question of the structural determinants of the tetrameric assembly of the DFF. It has been demonstrated that the CIDE-N domains of CAD and ICAD are essential for their dimerization (24, 32, 33). Therefore, we next examined the role of the CIDE-N domains in the formation of tetrameric DFF. First, we tested whether the N-terminally truncated ICAD-Myc lacking its CIDE-N domain (ΔCIDE-ICAD-Myc) retains its capacity to bind to CAD.

ΔCIDE-ICAD-Myc was co-expressed with CAD-HA in HeLa cells, and the complex formation was probed by co-immunoprecipitation. Although the expression level of ΔCIDE-ICAD-Myc was only moderately lower than ICAD-Myc (Fig. 5, *lanes 3* and *5*, *lower panel*), only ICAD, but not ΔCIDE-ICAD, was associated with CAD-HA (Fig. 5, *lanes 6* and *4*, *lower panel*). The expression level of CAD-HA in the presence of ΔCIDE-ICAD-Myc was significantly lower as compared with ICAD-Myc, consistent with the lack of CAD and ΔCIDE-ICAD-Myc interaction (Fig. 5, *lanes 3* and *5*, *top panel*). These results confirmed previous observations that the CIDE-N domain of ICAD is required for interaction with nuclease (24).

To assess whether the CIDE-N domain of CAD is necessary for the CAD/ICAD and CAD/CAD complex formation, HA-ICAD and FLAG-ICAD were co-expressed with ΔCIDE-CAD-Myc. Anti-HA antibody efficiently precipitated HA-ICAD (Fig. 6*A*, *upper panel*). Surprisingly, besides CAD-Myc, ΔCIDE-CAD-Myc was also co-precipitated with HA-ICAD, implying that N-terminally truncated CAD retains some of its binding to ICAD, though at somewhat lower efficiency (Fig. 6*A*, *lanes 4* and *6*, *middle panel*). The robust expression of ΔCIDE-CAD-Myc in the presence of heterologous ICAD suggests that the CIDE-N domain of CAD is not an absolute requirement for chaperone activity of ICAD on CAD folding (Fig. 6*A*, *lanes 3* and *5*, *upper* and *middle panel*). Importantly, replacement of CAD-Myc with ΔCIDE-CAD-Myc prevented the interaction between HA-ICAD and FLAG-ICAD (Fig. 6*A*, *lanes 4* and *6*, *lower panel*). The latter result was consistent with the hypothesis that CIDE-N of CAD is necessary for the dimerization of 2 CAD/ICAD complexes to form the tetrameric DFF. If this assumption is correct, ΔCIDE-CAD should not support the incorporation of 2 CAD molecules in the DFF. This was indeed the case. Whereas CAD-HA and CAD-Myc

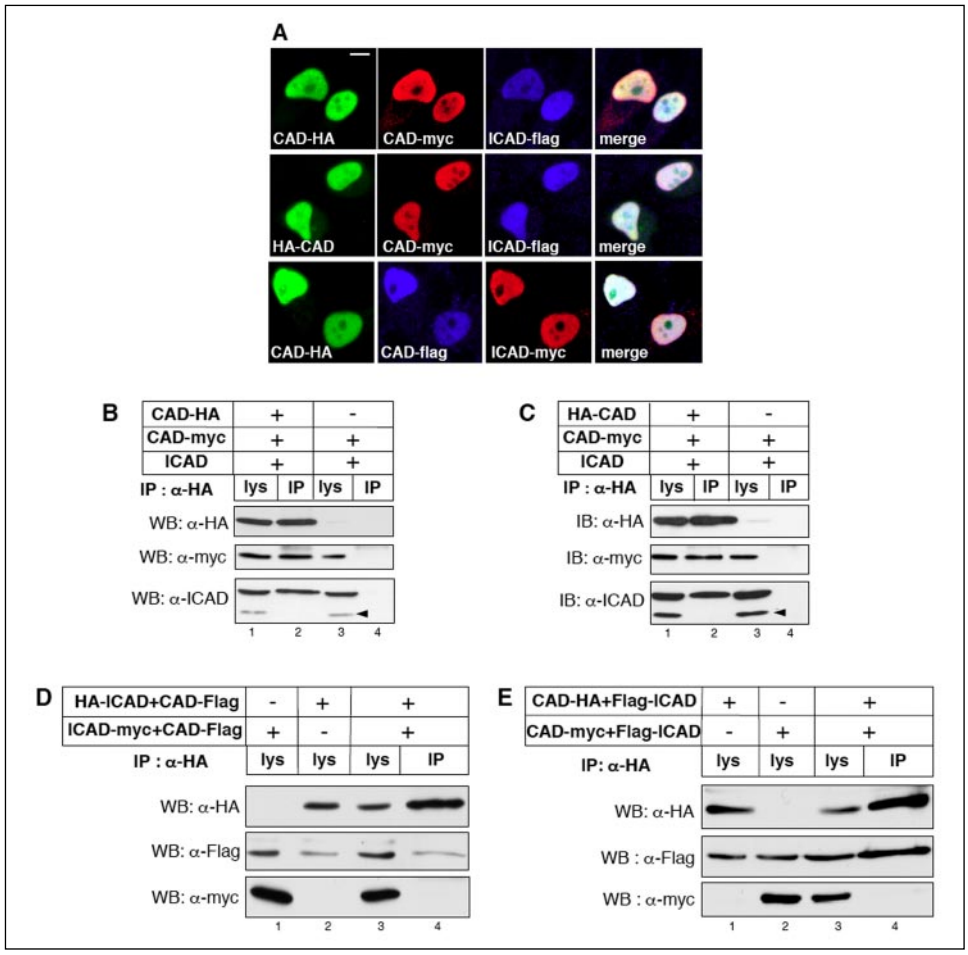

FIGURE 4. **CAD associates with CAD in the presence of ICAD.** *A*, indirect immunofluorescence of HeLa cells co-expressing triple-tagged DFF. Tagged CAD was transiently expressed with ICAD-FLAG or ICAD-Myc in HeLa cells. ICAD and CAD expressions were visualized by indirect immunostaining as described in the legend to Fig. 2*A*. *Bar*, 10 μM. *B* and *C*, dimerization of CAD in DFF. HeLa cells were co-transfected with the indicated constructs. CAD was immunoprecipitated with anti-HA antibody. 5% of the lysates (*lys*) and the precipitates (*IP*) were immunoblotted with the indicated antibodies. The polyclonal anti-ICAD antibody recognized both endogenous and exogenous human and ICAD-S (*bottom panel*, *lanes 1* and *3*, *arrowhead*). *D*, ICAD homodimerization does not occur *in vitro*. CAD-FLAG/HA-ICAD or CAD-FLAG/ICAD-Myc was co-transfected in HeLa cells. Cell lysates were pooled and incubated on ice for 1 h before immunoprecipitation with HA antibody. 5% of the individual or the combined lysate (*lys*), and the immunoprecipitates (*IP*) were blotted with the indicated antibodies. *E*, CAD homodimerization does not occur *in vitro*. CAD-Myc/FLAG-ICAD and CAD-HA/FLAG-ICAD were co-transfected in HeLa cells. Cell lysates were processed as described in *D*.

were efficiently co-precipitated in the presence of ICAD (Fig. 6*B*, *lane 4*, *upper* and *middle panels*), only a small amount of ΔCIDE-CAD-Myc was recovered in CAD-HA precipitates (Fig. 6*B*, *lane 2*, *upper* and *middle panels*). These results are in line with our conclusion that DFF in non-apoptotic cells consists of 2 CAD/ICAD heterodimers and suggest that their association requires the CIDE-N domain of CAD.

Domain Requirements of CAD for Mediating CAD-ICAD and ICAD-ICAD Interactions in Vivo—Although ΔCIDE-CAD retains its binding to ICAD, the formation of tetrameric DFF appears to be impaired (Fig. 6). To further investigate the structural requirements of dimerization (CAD/ICAD) and tetramerization (CAD/ICAD with CAD/ICAD), complex formation of ICAD with itself and with CAD was followed using C- and N-terminally truncated CAD variants (Fig. 7*A*). CAD truncations were designed based on sequence alignment of the human, mouse, chicken, and *Drosophila* CAD (dCAD), respecting the putative domain boundaries (34). CAD deletion mutants were fused in-frame to the EGFP (Ref. 29 and Fig. 7*A*).

To define the domain requirement of CAD for association with ICAD *in vivo*, ICAD-Myc co-precipitation was determined with the truncated CAD variants. The CIDE-N domain of CAD (residues 1–84) inefficiently bound ICAD (Fig. 7*B*, *lane 8*), compared with full-length (1–338) or truncated CAD-(1–278) (Fig. 7*B*, *lanes 2*, *6*, and *8*, *bottom panel*). The combination of N- and C-terminal truncations of CAD revealed that besides the CIDE-N domain, the C2 and the N-terminal of C3 domain seem to contribute to the stabilization of the CAD/ICAD association (Fig. 7*B*).

Next, the domain requirement of DFF dimerization was assessed, taking advantage of the CAD-dependent interaction of 2 ICADs in the

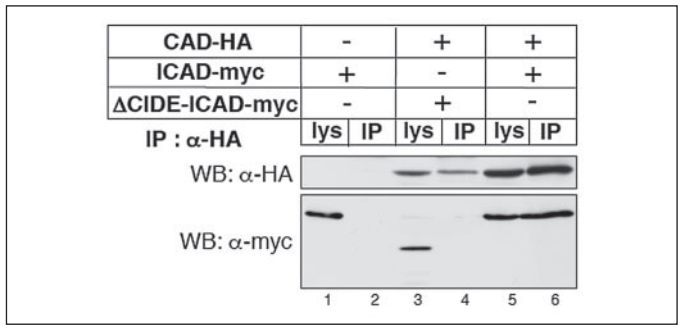

FIGURE 5. **The CIDE-N domain of ICAD is required for CAD binding.** The full-length or ICAD lacking the N-terminal CIDE-N domain was co-expressed with CAD-HA in HeLa cells. As control, cells were transfected with ICAD-Myc alone. CAD-HA was precipitated with anti-HA antibody. 5% of the lysate (*lys*) and precipitates (*IP*) were immunoblotted (*WB*) with the specified antibodies.

DFF (Figs. 2*B* and 6*A*). Truncated CAD-EGFP variants were co-expressed with ICAD-Myc and FLAG-ICAD, and the association of ICADs was measured. FLAG-ICAD was bound to ICAD-Myc only in the presence of CAD encompassing amino acid residues 1–278, but not residues 1–152 (Fig. 7*C*, *lanes 4* and *6*, *middle panel*). Thus, tetramerization of DFF requires both the C1 and C2 domains of CAD, whereas the C-terminal 50 amino acid residues are dispensable (Fig. 7*A*).

Oligomeric Structure of DFF in Apoptotic Cells—Next, the subunit composition of DFF was determined in HeLa cells undergoing programmed cell death. Staurosporine, a nonspecific protein kinase C inhibitor, was used to induce apoptosis (35). We confirmed that staurosporine-induced caspase-3 activation leads to the rapid proteolysis of

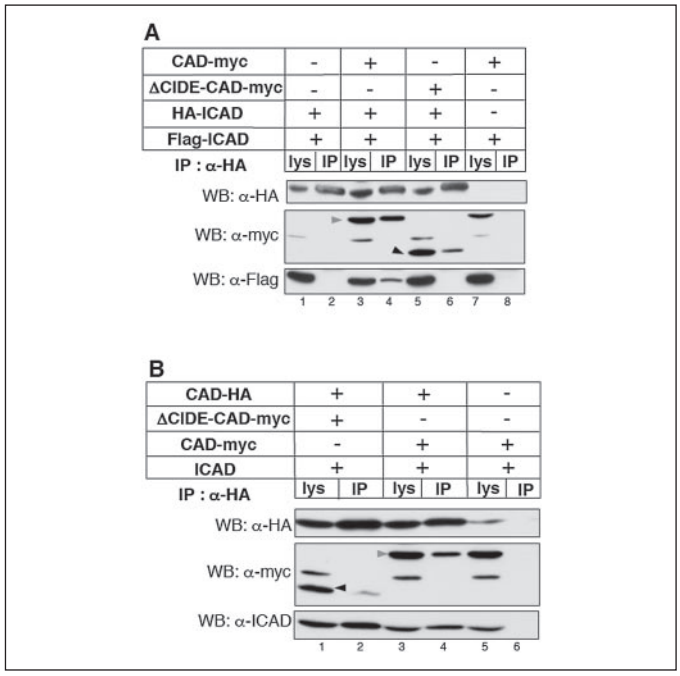

FIGURE 6. **The role of the CAD CIDE-N domain in the oligomerization state of the DFF.** *A*, ΔCIDE-N of CAD domain is required for the incorporation of two ICAD in DFF. HeLa cells were transfected with HA-ICAD and FLAG-ICAD with either CAD-Myc or ΔCIDE-CAD-Myc. Cells transfected with CAD-Myc and FLAG-ICAD without HA-ICAD were used as control (*lanes 7* and *8*). Cell lysates were immunoprecipitated with HA antibody. 5% of the cell lysates (*lys*) and precipitates (*IP*) were blotted (*WB*) with the indicated antibodies. ICAD-FLAG was co-precipitated with HA-ICAD only in the presence of CAD-Myc. *Black arrowhead*, ΔCIDE-CAD; *gray arrowhead*, CAD. *B*, ΔCIDE-CAD binds to ICAD, but not to CAD. HeLa cells were transfected either with CAD-HA or ΔCIDE-CAD-Myc together with CAD-Myc and ICAD. Cell lysates were immunoprecipitated as in *A*. Cells transfected with carrier DNA instead of CAD-HA were used as control (*lanes 5* and *6*).

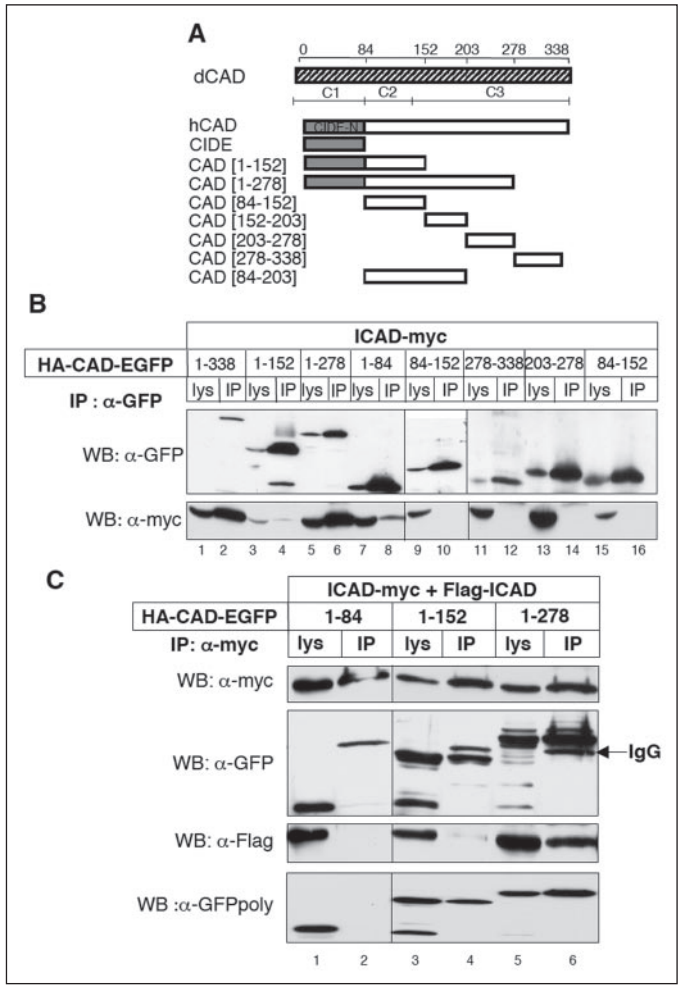

FIGURE 7. **The CIDE-N domain of CAD is necessary, but not sufficient to promote the incorporation of two ICADs in DFF.** *A*, deletion mutants of CADs were fused to the N terminus of the EGFP. Progressively truncated CADs, with the indicated amino acid residues, were fused in-frame to EGFP. Truncated variants of the human CAD were designed based on sequence alignment of the human, mouse, chicken, and *Drosophila* CAD, respecting putative domains boundaries (40). The domain structures of CAD (C1, C2, and C3) as described (28) are indicated. *B*, CIDE-N domain of CAD is not sufficient for efficient heterodimerization of ICAD and CAD. HeLa cells were transiently transfected with the CAD deletion mutants and with ICAD-Myc. CAD was precipitated with anti-GFP antibody. The abundance of CAD fusion proteins (*top panel*) and ICAD-Myc (*bottom panel*) was measured in cell lysates (*lys*) and immunoprecipitates (*IP*). *C*, structural requirement of CAD for inducing oligomerization of ICAD in DFF. HeLa cells were transfected with the C terminus CAD deletion mutants that interact with ICAD (see *B*), together with ICAD-Myc and ICAD-FLAG. Cell lysates were immunoprecipitated with anti-Myc antibody, and 5% of the cell lysates and the precipitates were blotted with indicated antibodies.

ICAD and concomitant DNA ladder formation in HeLa cells (supplemental materials Fig. S1*A* and Ref. 29). The majority of exogenous and endogenous ICAD was cleaved after 2.5 h of staurosporine treatment (supplemental materials Fig. S1*A* and compare *lower panels* of Fig. 8*A*, *lanes 3* and *5*), implying that most of the cellular CAD was activated.

To assess oligomerization of CAD in activated DFF, HeLa cells, transiently co-expressing CAD-HA and CAD-Myc were treated with staurosporine for 2 h, and CAD-HA was immunoisolated. A significant amount of CAD-Myc was recovered in the CAD-HA precipitates relative to its cellular content, whereas >85% of ICAD was degraded (Fig. 8*A*, *lane 6*, *middle panel*). This observation indicates that activated DFF contains at least 2 CAD molecules.

The oligomerization of activated CAD was further examined in HeLa S-100 fraction. First, we verified that endogenous CAD and ICAD were efficiently extracted and that ICAD was degraded in the presence of recombinant caspase-3 (supplemental materials, Fig. S1*B*). S-100 fraction of cells expressing either CAD-HA/ICAD-FLAG or CAD-Myc/ICAD-FLAG were combined, incubated with caspase-3, and immunoprecipitated with anti-HA antibody. Caspase-3 induced the complete degradation of ICAD-FLAG (Fig. 8*B*, *lane 4*, *lower panel*). Though degradation of CAD-HA was evident, the immunoprecipitated CAD-HA was associated with CAD-Myc, but not with ICAD-FLAG. These observations highlight that activated CAD complex originates from distinct inactive DFF complexes (Fig. 8*B*, *lanes 5* and *6*, *middle panel*). Similar results were obtained with differently tagged CAD and ICAD (data not shown) further supporting the oligomeric structure of activated CAD.

To substantiate the oligomerization state of CAD, the molecular mass of activated DFF was measured by size-exclusion chromatography in cell extracts obtained from staurosporine-induced apoptotic HeLa cells. Gel filtration and immunoblotting revealed that the molecular mass of endogenous CAD was ~80–160 kDa (Fig. 8*C*). This is consistent with the co-precipitation data and confirms that activated DFF incorporates more than 1 CAD molecule and, perhaps, other polypeptides as well. Activated CAD-HA was also separated as ~110–190-kDa complexes from HeLa cells, expressing CAD-HA/ICAD-Myc (Fig. 8*D*, *top panel*). None or negligible amounts of ICAD were detectable in fractions containing CAD, indicating that the caspase-3-dependent cleavage of ICAD-Myc, as well as ICAD was virtually complete (Fig. 8, *C* and *D*, *lower panels*). We were unable to confirm the formation of large macromolecular complexes of CAD with >1 MDa masses, because neither endogenous nor the exogenous CAD appeared in the void volume (Fig. 8, *C* and *D*). Likewise, no significant amount of monomeric CAD was detected. Control experiments demonstrated that extraction of CAD from nuclei was complete (data not shown). Aggregated CAD

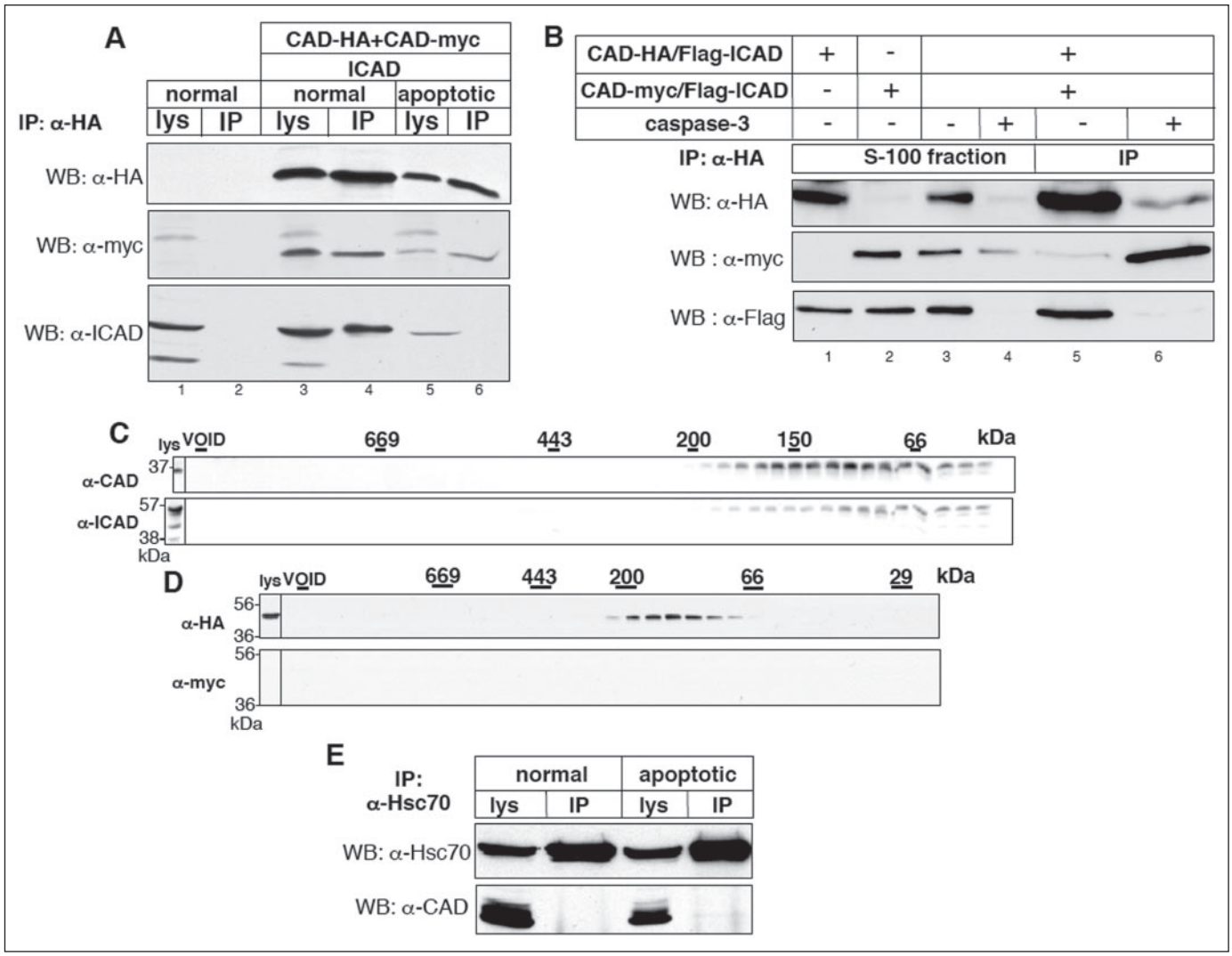

FIGURE 8. **Oligomerization of CAD in apoptotic cells.** *A*, CAD-HA associates with CAD-Myc in apoptotic cells. HeLa cells were co-transfected with CAD-HA and CAD-Myc together with ICAD. Non-transfected cells were used as controls (*lanes 1* and *2*). Lysates of dividing cells (*lanes 3* and *4*) or cells exposed to 2 μM staurosporine for 2 h (*lanes 5* and *6*) were precipitated with anti-HA antibody. 5% of the lysates (*lys*) and precipitates (*IP*) were blotted (*WB*) with indicated antibodies. The polyclonal anti-ICAD antibody recognized both endogenous and exogenous human and ICAD-S (*bottom panel*, *lanes 1* and *3*). *B*, CAD derived from distinct DFF complexes associates following caspase-3 cleavage of ICAD *in vitro*. Cell extracts were prepared from HeLa cells, expressing CAD-HA and FLAG-ICAD or CAD-Myc, and FLAG-ICAD (see "Materials and Methods"). Combined extracts were incubated with active caspase-3 (1 unit/μg of protein) for 1 h at room temperature before immunoprecipitation with anti-HA antibody, and 5% of the cell lysates and the precipitates were blotted with the indicated antibodies. *C* and *D*, analysis of endogenous and heterologous DFF molecular mass by size-exclusion chromatography in apoptotic cells. Non-transfected (*C*) or CAD-HA/ICAD-Myc-expressing (*D*) HeLa cells were treated with 2 μM staurosporine for 2 h. Cell lysates were fractionated by size-exclusion chromatography as described under "Materials and Methods." Fractions were probed by Western blot analysis with anti-hCAD, anti-hICAD, anti-HA, and anti-Myc antibodies, as indicated and described in the legend to Fig. 1. *E*, CAD does not bind to immunoisolated Hsc/Hsp70 in normal and apoptotic cells. Apoptosis was induced for 2 h with 2 μM staurosporine. After immunoprecipitation of the lysates with anti-Hsc/Hsp70 antibody, precipitates were probed with anti-Hsc/Hsp70 (*upper panel*) and anti-CAD (*lower panel*) antibodies. 5% of the total lysates was loaded as control.

could not be recovered from insoluble fractions or from the pellet obtained by ultracentrifugation (data not shown). Finally, similar results were obtained on activated CAD, following the complete cleavage of ICAD by recombinant caspase-3 in the isolated HeLa S-100 fraction. Size-exclusion chromatography and immunoblotting showed that the molecular mass of the *in vitro* activated CAD was ~90–120 kDa (supplemental Fig. S2), consistent with its limited oligomerization also detected in staurosporine-treated cells. The complete proteolysis of ICAD *in vitro* was verified by immunoblotting (supplemental Fig. S2, *lane 1 versus 2*)

Heterologously expressed CAD binds to overexpressed Hsp70 following the activation of DFF (36). To examine whether endogenous Hsp/Hsc70 is incorporated into the activated DFF, we probed Hsp/Hsc70 immunoprecipitates for the presence of CAD (Fig. 8*E*). Although a high amount of Hsp/Hsc70 was isolated from normal and apoptotic HeLa cells, endogenous CAD could not be detected in the Hsp/Hsc70 precipitates (Fig. 8*E*, *lower panel*). Co-precipitation of CAD was also unsuccessful when the ATP content of cell lysates was depleted by apyrase to prevent the dissociation of chaperones from their substrates (data not shown) (37). Whereas we cannot discount the possibility that one or more presently unidentified polypeptides are binding to the activated DFF (3), our results indicate that both the endogenous and exogenous CAD undergo limited homo-oligomerization in apoptotic cells.

DISCUSSION

According to the prevailing model, DFF exists as a heterodimer, composed of one ICAD and one CAD molecule expressed in the nucleus of non-apoptotic cells (27). Activation of caspase-3 or -7 causes the dissociation of ICAD and the formation of the activated CAD, forming large homo-oligomeric complexes (27). Based on a combination of *in vivo*

and *in vitro* approaches, utilizing both endogenous and ICAD and CAD, we propose an alternative model, suggesting that the inactive DFF is composed of a heterotetramer $(CAD/ICAD)_2$, which undergoes limited homo-oligomerization during apoptosis. In addition, some of the structural cues of DFF complex formation have been established.

Size-exclusion chromatography indicated that both endogenous and heterologously expressed DFF have a molecular mass of ~150–200 kDa, which is 2-fold larger than the apparent M_r of the CAD/ICAD heterodimer (10). Utilizing a panel of epitope-tagged CAD and ICAD molecules, co-immunoprecipitation and BRET assays, we demonstrated that the inactive DFF contains 2 ICAD and 2 CAD molecules, providing a plausible explanation for the observed M_r of DFF (Fig. 1). Whereas the co-precipitation results cannot rule out the co-existence of the trimeric $CAD/(ICAD)_2$ and $(CAD)_2/ICAD$ *in vivo*, this is highly unlikely, considering that M_r of these heterotrimers would be significantly smaller (~120–130 kDa) than the observed M_r of DFF (~150–200 kDa). Additional considerations also support the $(CAD/ICAD)_2$ tetrameric subunit structure of DFF in non-apoptotic cells. First, the diffusional mobility of DFF is comparable to the freely diffusing EGFP, determined by fluorescence recovery after photobleaching (FRAP) (29). This implies that incorporation of polypeptides with high affinity binding to chromatin is unlikely. Whereas chromatin-binding proteins (*e.g.* histone H1 and HMG2) were implicated in complex formation with DFF (3), these DNA-binding proteins have nearly 2 orders of magnitude slower diffusion coefficients than DFF (29, 38, 39). Second, molecular mass determination of heterologously expressed *Drosophila melanogaster* DFF, suggested that dCAD (M_r ~52 kDa) and dICAD/DREP-1 (M_r ~46 kDa) form a ~145-kDa complex in non-apoptotic COS-1 cells, although the stoichiometry of this complex has not been determined (40). Third, ICAD binds co-translationally to the nascent polypeptide of CAD to exert its chaperone function (19), supporting the idea that DFF contains stoichiometric amounts of CAD and ICAD. Finally, and most importantly, demonstration of the CAD-dependent ICAD-ICAD interaction in living cells by the BRET technique (Fig. 3) substantiated the notion that DFF contains at least two ICAD molecules. Because of the obligatory cotranslational association of CAD with ICAD, this would favor the $(ICAD/CAD)_2$ subunit composition of DFF in its native environment, the nucleosol.

Our conclusion that DFF consists of a heterotetramer in dividing cells is also consistent with 2 earlier studies, monitoring the apparent M_r of ICAD. Liu *et al.* (8) used endogenous DFF isolated by Mono Q and gel filtration column purification and estimated that the apparent M_r of DFF was >100 kDa. McCarty *et al.* (41) reported that the DFF formed a ~120–1600-kDa complex, purified by gel filtration. Whereas these studies did not provide an explanation for the subunit composition of the inactive DFF, their results are in-line with the molecular mass determination of both endogenous and exogenous DFF reported here. Structural destabilization and dissociation of the heterotetrameric DFF may have occurred during the long purification procedures of DFF and led to the appearance of CAD/ICAD as a heterodimer (10). In addition, expression of DFF in bacteria may render tetramerization unfavorable for presently unknown reasons (27).

The tetrameric subunit composition of DFF may have biological advantage. Tetramerization may enhance the nuclear targeting of the DFF, in light of the additive effect of multiple NLS (15). It is also plausible that co-expression of 2 ICADs in DFF constitutes a safeguard against accidental activation of the potentially harmful DNase in proliferating cells. Finally, the proximity of 2 CAD molecules in the DFF may facilitate their conformational rearrangement, to attain the enzymatically active homodimer, as determined by analyzing the crystal structure of CAD (28).

Our gel filtration experiments as well as previous studies suggested that ICAD is expressed in molar excess of CAD (21). In the absence of CAD, ICAD was eluted around 45–70 kDa, suggesting that ICAD is engaged in homo- or heteromeric protein-protein interactions. Co-precipitation studies, however, ruled out that overexpressed ICAD binds to ICAD or ICAD-S in the absence of exogenous CAD (Fig. 2) (33), suggesting that direct ICAD/ICAD interaction cannot account for the tetramerization of DFF. Indeed, deletion of CIDE-N in CAD prevented the incorporation of 2 ICADs into the DFF, whereas the heterodimerization of CAD with ICAD was maintained (Fig. 6). This suggests that the association of 2 CAD/ICAD complexes is mediated, at least in part, by the CIDE-N domains of CAD.

Molecular mass determination by gel filtration (Fig. 8) and native gel electrophoresis (data not shown) showed that active CAD does not form megadalton size complexes, as reported for the recombinant nuclease (9, 21, 42). The apparent molecular mass of activated CAD with the co-immunoprecipitation results supports the model that activated DFF contains at least 2 and up to 4 CAD subunits. These results partially overlap with the data of Widlak *et al.* (21) demonstrating that the smallest oligomer of activated CAD is a tetramer, although it predominantly forms large homo-oligomers. We were unable to demonstrate that endogenous Hsp70 is incorporated into the active DFF, as suggested by precipitation studies using overexpressed Hsp70 (36). Whereas the dissociation of mega dalton size CAD complexes cannot be discounted during the short chromatography, this is unlikely because complex formation of endogenous Hsp70 with nascent polypeptide chains in the 100–600-kDa range were detected (data not shown). These results, with the *in vitro* assembly of activated CAD complexes containing CAD-HA and CAD-Myc, are consistent with the hypothesis that following the cleavage of $ICAD_2$, the dimeric CAD assembles into a tetramer. We speculate that the activated CAD instability in diluted cytosol may explain the excessive oligomerization observed *in vitro,* which is not unexpected in light of the documented aggregation tendency of newly synthesized CAD in the absence of ICAD (19).

Recent biochemical and structural evidence suggest that homodimerization of active CAD ensures the structural requirement for the DNase to recognize the internucleosomal DNA as its substrate (28, 43). Our *in vivo* data are in accordance with these results and confirm the notion that activated CAD cleaves the chromosomal DNA as a small oligomer. Limited oligomerization may provide structural scaffold for the activated DNase, substituting for the stabilizing effect of ICAD following its caspase-3-dependent cleavage.

We envision that CAD oligomerization may represent a modulatory mechanism in the activation of DFF in apoptotic cells. One scenario is that following the release of a single CAD from the heterotetrameric DFF, CAD binds to another monomeric CAD and forms the active nuclease with other, presently unknown polypeptide(s). Alternatively, following the cleavage of ICAD, CAD persists as a trimer $(CAD_2/ICAD)$. The cleavage of the second ICAD will render the dimeric CAD competent to form the dimeric or tetrameric form. Both models imply that the DNase activation requires the proteolysis of sufficient amount of ICAD that would lead to the oligomerization of CAD (as $2\times(CAD)_2$ or $2\times CAD$) in a relatively short period of time. This mechanism is reminiscent of the cooperative activation of caspases, implicated in the initiation of programmed cell death (14), and may serve as an all-or-none switch in the irreversible process of chromosomal DNA degradation.

In summary, our results provided evidence for the heterotetrameric structure of DFF $(CAD/ICAD)_2$, in the nucleus of dividing cells. The

dimerization of two CAD/ICAD complexes requires the CIDE-N domain of CAD, which likely mediates the limited oligomeric assembly of CAD in activated DFF. The oligomeric structure of the inactive and activated DFF may not only protect the cell against inadvertent activation of the apoptotic nuclease, but also contributes to the synchronous and cooperative activation of CAD during programmed cell death.

Acknowledgments—We thank R. Halenbeck and S. Nagata for generously providing expression plasmids. We are grateful for the helpful advice of M. Bouvier in setting up the BRET assay.

REFERENCES

1. Nicholson, D. W. (1999) *Cell Death Differ.* **6,** 1028–1042
2. Hanayama, R., Tanaka, M., Miwa, K., Shinohara, A., Iwamatsu, A., and Nagata, S. (2002) *Nature* **417,** 182–187
3. Zhang, J., and Xu, M. (2002) *Trends Cell Biol.* **12,** 84–89
4. Herrmann, M., Voll, R., Zoller, O., Hagenhofer, M., Ponner, B., and Kalden, J. (1998) *Arthr. Rheum.* **41,** 1241–1250
5. Scovassi, A., and Torriglia, A. (2003) *Eur. J. Histochem.* **47,** 185–194
6. Nagata, S. (2000) *Exp. Cell Res.* **256,** 12–18
7. Nagata, S. (2005) *Annu. Rev. Immunol.* **23,** 853–875
8. Liu, X., Zou, H., Slaughter, C., and Wang, X. (1997) *Cell* **89,** 175–184
9. Liu, X., Li, P., Widlak, P., Zou, H., Luo, X., Garrard, W. T., and Wang, X. (1998) *Proc. Natl. Acad. Sci. U. S. A.* **95,** 8461–8466
10. Enari, M., Sakahira, H., Yokoyama, H., Okawa, K., Iwamatsu, A., and Nagata, S. (1998) *Nature* **391,** 43–50
11. Sakahira, H., Enari, M., and Nagata, S. (1998) *Nature* **391,** 96–99
12. Halenbeck, R., MacDonald, H., Roulston, A., Chen, T. T., Conroy, L., and Williams, L. T. (1998) *Curr. Biol.* **8,** 537–540
13. Liu, X., Zou, H., Widlack, P., Garrard, W., and Wang, X. (1999) *J. Biol. Chem.* **274,** 13836–13840
14. Renatus, M., Stennicke, H. R., Scott, F. L., Liddington, R. C., and Salvesen, G. S. (2001) *Proc. Natl. Acad. Sci. U. S. A.* **98,** 14250–14255
15. Lechardeur, D., Drzymala, L., Sharma, M., Pacia, J., Hicks, C., Usmani, N., Zylka, D., Rommens, J., and Lukacs, G. L. (2000) *J. Cell Biol.* **150,** 321–334
16. Samejima, K., and Earnshaw, W. C. (1998) *Exp. Cell Res.* **243,** 453–459
17. Sholz, S. R., Korn, C., Gimadutdinow, O., Knoblauch, M., Pingoud, A., and Meiss, G. (2002) *Nucleic Acids Res.* **30,** 3045–3051
18. Widlak, P., Li, P., Wang, X., and Garrard, W. T. (2000) *J. Biol. Chem.* **275,** 8226–8232
19. Sakahira, H., and Nagata, S. (2002) *J. Biol. Chem.* **277,** 3364–3370
20. Sakahira, H., Iwamatsu, A., and Nagata, S. (2000) *J. Biol. Chem.* **275,** 8091–8096
21. Widlak, P., Lanuszewska, J., Cary, R. B., and Garrard, W. T. (2003) *J. Biol. Chem.* **278,** 26915–26922
22. Toh, Y. T., Wang, X., and Li, P. (1998) *Biochem. Biophy. Res. Comm.* **250,** 598–601
23. Durrieu, F., Samejima, K., Fortune, J. M., Kandels-Lewis, S., Osheroff, N., and Earnshaw, W. C. (2000) *Curr. Biol.* **10,** 923–926
24. Inohara, N., Koseki, T., Chen, S., Benedict, M. A., and Nunez, G. (1999) *J. Biol. Chem.* **274,** 270–274
25. Meiss, G., Scholz, S. R., Korn, C., Gimadutdinow, O., and Pingoud, A. (2001) *Nucleic Acids Res.* **29,** 3901–3909
26. Zhou, P., Lugovskoy, A. A., McCarty, J. S., Li, P., and Wagner, G. (2001) *Proc. Natl. Acad. Sci. U. S. A.* **98,** 6051–6055
27. Widlak, P., and Garrard, W. T. (2005) *J. Cell Biochem.* **94,** 1078–1087
28. Woo, E.-J., Kim, Y.-G., Kim, M.-S., Han, W., Shin, S., Robinson, H., Park, S.-Y., and Oh, B.-H. (2004) *Mol. Cell* **14,** 531–539
29. Lechardeur, D., Xu, M., and Lukacs, G. L. (2004) *J. Cell Biol.* **167,** 851–862
30. Mukae, N., Enari, M., Sakahira, H., Fukuda, Y., Inazawa, J., and Toh, H. (1998) *Proc. Natl. Acad. Sci. U. S. A.* **95,** 9123–9128
31. Perroy, J., Pontier, S., Charest, P. G., Aubry, M., and Bouvier, M. (2004) *Nature Met.* **1,** 203–208
32. Otomo, T., Sakahira, H., Uegaki, K., Nagata, S., and Yamazaki, T. (2000) *Nat. Struct. Biol.* **7,** 658–662
33. Lugovskoy, A., and Zhou, P., Chou, J. J, McCarty, J. S, Li, P., and Wagner, G. (1999) *Cell* **99,** 747–755
34. Mukae, N., Yokoyama, H., Yokokura, T., Sakoyama, Y., Sakahira, H., and Nagata, S. (2000) *J. Biol. Chem.* **275,** 21402–21408
35. Samuelsson, M., Pazirandeh, A., and Okret, S. (2002) *Biochem. Biophy. Res. Commun.* **296,** 702
36. Liu, Q.-L., Kishi, H., Ohtsuka, K., and Muraguchi, A. (2003) *Blood* **102,** 1788–1796
37. Kampinga, H. H., Kanon, B., Salomons, F. A., Kabakov, A. E., and Patterson, C. (2003) *Mol. Biol. Cell* **23,** 4948–4958
38. Misteli, T., Gunjan, A., Hock, R., Bustin, M., and Brown, D. T. (2000) *Nature* **408,** 877–881
39. Kimura, H., and Cook, P. R. (2001) *J. Cell Biol.* **153,** 1341–1353
40. Yokoyama, H., Mukae, N., Sakahira, H., Okawa, K., Iwamatsu, A., and Nagata, S. (2000) *J. Biol. Chem.* **275,** 12978–12986
41. McCarty, J., Toh, S., and Li, P. (1999) *Biochem. Biophys. Res. Commun.* **264,** 181–185
42. Widlak, P., and Garrard, W. T. (2001) *Mol. Cell Biochem.* **218,** 125–130
43. Korn, C., Scholz, S. R., Gimadutdinow, O., Lurz, R., Pingoud, A., and Meiss, G. (2005) *J. Biol. Chem.* **280,** 6005–6015

Oligomerization State of the DNA Fragmentation Factor in Normal and Apoptotic Cells

Delphine Lechardeur, Sam Dougaparsad, Csilla Nemes and Gergely L. Lukacs

J. Biol. Chem. 2005, 280:40216-40225.
doi: 10.1074/jbc.M502220200 originally published online October 3, 2005
